Journal of Metals, Materials and Minerals, Vol. 30, No. 4, pp. 68-78, 2020

Laser powder bed fusion of Ti6Al4V lattice structures and their applications

Thywill Cephas DZOGBEWU*

Department of Mechanical and Mechatronics Engineering, Central University of Technology, Free State, 9301 Bloemfontein, South Africa

***Corresponding author e-mail:** tdzogbewu@cut.ac.za

Received date:
1 May 2020
Revised date
13 September 2020
Accepted date:
19 September 2020

Keywords:
LPBF;
Ti6Al4V;
Lattice structures;
Mechanical properties;
Microstructure

Abstract

The study focused on producing lattice structures using rhombic and diagonal nodes and indicating their logical biomedical and engineering applications. Laser powder bed fusion manufacturing technology a subset of additive manufacturing was used to manufacture the lattice structures with different struts geometry. Average elastic modulus value of 5.3±0.2 GPa was obtained for the rhombic lattice structures and 5.1±0.1 GPa for the diagonal lattice structures. Generally, the mechanical properties of the lattice structures produced could be logically considered suitable for biomedical and engineering applications. The mechanical properties of the lattice structures could be fine-tuned for a specific engineering or biomedical applications by varying the lattice properties of the lattice structures.

1. Introduction

Ti6Al4V is a generic alloy which had widespread application in the engineering, surgical and biomedical industries and has become a reference metallic material in ASTM F standards [1], due to its unique mechanical and biocompatible properties [2]. Most researchers have focused on optimizing the laser powder bed fusion (LPBF) process to manufacture dense Ti6Al4V parts [3-5], but more recently great attention has been given to manufacturing low-density Ti6Al4V lattice structures for engineering and biomedical applications [6,7], due to their unique loading bearing and multifunctional characteristics.

Lattice structures can be described as a periodic array of cells making up of struts connecting between two nodes which are rigidly bonded [8,9]. Lattice structures are ultralightweight metamaterials with high specific strength, high specific rigidity, high durability, high energy absorption rate, and thermal protection [8,10], therefore fulfill multifunctional requirements for most engineering and biomedical applications.

The mechanical behavior of a lattice material is mainly dependent on its internal architecture, the relative density, strut aspect ratio (radius/length), unit cell geometric configuration, unit-cell size, properties of parent material, and rate of loading. By changing the spatial configuration of struts and/or strut diameters, different geometries with different material properties can be produced. Thus, the mechanical properties of lattice structures can be tuned for a specific application [11,12].

However, with the conventional methods of manufacturing such as sheet forming, perforated/slotted, sheet folding, extrusion, wire assembly, and investment casting methods it was very difficult and almost impossible to produce periodic lattice structures with complex tailored geometrical configurations [13]. The cell size of most of the lattice structures produce using the conventional methods were of the order of centimeters [7], due to the inherent limitations of the classical methods to produce complex lattice structures. The classical methods require multiple processing steps of perforating and folding from metal sheets. These steps are time-consuming and allow the production of a limited amount of lattice geometries [15].

However, with the rapid development in manufacturing technology and the emergence of additive manufacturing (AM) technology such as laser powder bed fusion manufacturing technology, it is possible to produce lattice materials with struts diameter ranging from submicron's to millimeters [16] which would permit the production of functional lattice structures based on position and geometrical requirements for each specific application [12].

LPBF manufacturing technology is an eco-design topology optimization technology that allows very complex shapes to be created monolithically additively, as opposed to the conventional methods of subtractive manufacturing. LPBF manufacturing technology is considered a renaissance of the manufacturing industry because it provides almost unchallenged freedom of design. The high degree of freedom offered by the LPBF technology of building complex lattice structures with tailored geometries would enable the novel development of lightweight customized biomimetic structures and functional engineering structures [17].

Despite the remarkable celebration of Ti6Al4V alloy for biomedical applications, issues of stress shielding effect (the miss-match between the elastic modulus of the dense Ti6Al4V implants and the bone tissue) [2,6] leading to implant failure [12] are still unresolved. This is due to replacing damaged bone tissues of low elastic modulus (Table 4) with dense Ti6Al4V alloy which has a high elastic modulus (110 GPa) [2]. To avoid the miss-match between

the elastic modulus of the metallic implant and the bone tissues, biometric structures such as lattice structures of low elastic modulus (Table 3) are required. Ashby *et al.* [18], have already pointed out that when nature builds, she generally uses cellular materials; wood, bone, coral, but when modern man builds large load-bearing structures, he uses dense solids; steel, concrete, glass. There must be a reason why mother nature uses cellular structures. Mimicking mother nature by manufacturing the Ti6Al4V implants using cellular structures topology instead of the dense Ti6Al4V implants might probably solve the stress shielding effects issues. In the quest to mimic nature as the most ideal model, the current research is focused on using the versatility of LPBF technology to manufacture lattice structures of intricate shapes with mechanical properties that might be comparable to that of bone tissue to avoid stress shielding effect. Also, the ever-increasing demand for developing lightweight structural materials for automotive and aerospace applications could be solved by using lattice structures to build some of the components of aircraft and automobiles parts [15], since lattice structures are ultralightweight metamaterials and their mechanical properties can be fine-tuned by changing the spatial configuration of the lattices. The current research, therefore, seeks to produce lattice structures with intricate shapes and investigate their mechanical properties and elucidate the possible biomedical and engineering applications of the LPBF manufactured lattice structures based on the obtained mechanical properties.

2. Experimental

2.1 The CAD models

The nodes (unit cells-Figure 1) are the basic unit building blocks of the lattice structures. Rhombic and diagonal nodes were selected for the study partly because they can be easily manufactured by most AM technology including LPBF [15] and as lattice structures, they could create rough surfaces, to stimulate bone ingrowth (osseointegration), to mimic bone properties in order to avoid the stress-shielding effect [12], excellent performance and multi-functionality while reducing weight for engineering applications [9,10]. The lattice structures were generated by repeating the unit cells in three dimensions along the x, y, and z-axis. The samples were designed with 5 unit cells of a rhombic node (Figure 1(a)) and 5 unit cells of the body diagonal node (Figure 1(b)) of 50% volume fraction porosity. Volume fraction was defined as the volume percentage of solid material in the CAD cellular lattice structure. The cell topology of each of the structures is identical intact to ensure uniformity throughout the lattice. Five replications of each node (5 x 5 x 5) length x breadth x height - were oriented vertically in the ZYX direction. The strut sizes of the samples were 1.317 and 1.669 mm for rhombic and diagonal structures, respectively. The struts sizes and the volume fractions of the samples were chosen to mimic the orthotropic properties of the human bone as reported in the literature [12] and any possible engineering applications.

The model samples (Figure 1) have strengthened edges to avert the effect of edge effects which is normally prevalent in compressive mechanical testing of lattice structures. The strengthened edges would prevent localization of the stresses and strains on the edges under a compressive load and distribute the load more extensively and evenly [19].

2.2 Manufacturing of the lattice structures

The Electro-Optical System (EOS M280), a direct metal laser sintering (DMLS) machine was used for manufacturing the lattice structures. The machine mainly comprises a process chamber with a recoating system, computer control elevating systems, platform heating module, an optical system equipped with 400 W fiber laser, a process gas management system and a process computer with control software.

Spherical argon atomized Ti6Al4V (ELI) powder procured from TLS Technik was used. The elemental composition of the powder in weight percent (wt%) is presented in Tabel 1.

The 10^{th}, 50^{th} and 90^{th} percentiles of equivalent diameter (weighted by volume) of the powder particles were d_{10}=13 µm, d_{50}=23 µm and d_{90}=37 µm. The substrate and powder materials were similar in chemical composition. Argon was used as the protective atmosphere; the oxygen level in the chamber was 0.07-0.1%. The lattice structures were manufactured with optimum process parameters; laser power of 170 W, scanning speed of 1.25 $m \cdot s^{-1}$, hatch distance of 80 µm and powder layer thickness of 30 µm with zigzag scanning strategy [20]**.** The laser spot diameter was 80 µm. Four samples were manufactured for each type of the lattice structures and coded R1, R2, R3, and R4 for the rhombic lattice structures and D1, D2, D3, and D4 for the diagonal lattice structures. The samples were stress relieve in Ar atmosphere at a temperature of 650°C for 3 h and were cut from the based plates using electrical discharge machining. The samples were cleaned in an ultrasonic bath to remove the "loose attached" powder residues.

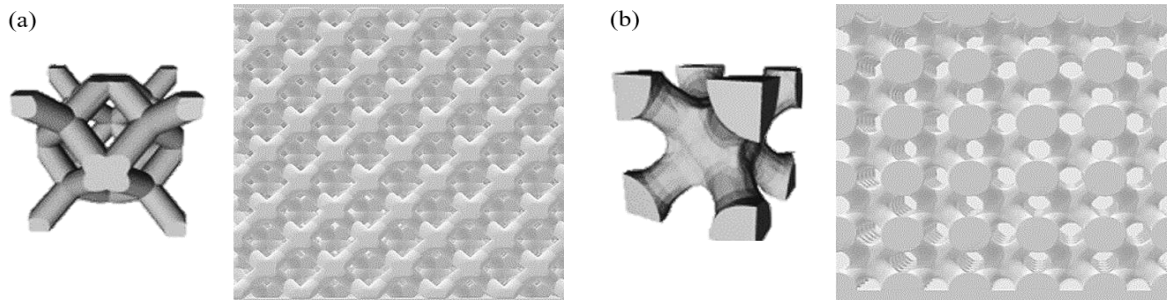

Figure 1. (a) Rhombic node and its lattice CAD model and (b) Diagonal node and its lattice CAD model.

Table 1. Elemental composition of the Ti6Al4V.

Element	Ti	Al	V	O	N	H	Fe	C	Y
Content (wt%)	Bal	6.34	3.94	0.058	0.006	0.001	0.025	0.006	0.001

2.3 Compressive test

MTS Criterion Model 43 Electromechanical Universal Test System machine was used for the compressive test. The samples were uniaxially compressed such that the top surface area of the lattice structures was in direct contact with the head of the testing machine. The compressive stress was determined as the ratio of the load (30 kN max load cell) to the top surface of the lattice structures at a strain rate of 0.3 $mm \cdot min^{-1}$. A total of four specimens were tested for each type of lattice structure, based on the ISO 13314 testing standard [21].

2.4 Metallurgical preparation of the samples

The cross-sections of the nodes of the lattice structures were prepared for metallographic studies using standard metallography procedures as demonstrated in the literature [23,24]. The samples were ground on 3000 SiC paper, polished with colloidal silica, and etched with Kroll's reagent (5 ml of HNO_3 + 10 ml of HF (48% concentration) + 85 ml H_2O). ZEISS Axio Scope. A1 Optical Microscope was used for the optical analysis. The surface morphology of the lattice structures was examined with a scanning electron microscope (JEOL JSM-7800F SEM) operated at a voltage of 15 kV.

3. Results and discussion

3.1 Mechanical analysis of the lattice structures

From the CAD models (Figure 1), the LPBF lattice structures were manufactured (Figure 2) for the study. The accuracy of the struts was investigated to determine if the geometry of the manufactured samples correspond to the CAD models. The struts sizes were measured and there was no significant differences between the struts of the CAD models and the manufactured samples. The struts size for rhombic lattice structure manufactured samples was 1.329±0.184 mm and 1.699±0.198 mm for the diagonal lattice structure. It could be inferred from this observation that the LPBF technology is attaining maturity and can be used to manufacture intricate shapes of thin walls with geometrical accuracy. This observation corresponds to the experimental results of Yadroitsev *et al*. [25]. They focused on manufacturing DMLS customized filters (lattice structures) of micron-sized channels and reported no significant variation between the CAD model and the manufactured DMLS thin walls (filters). A similar observation was demonstrated by Ma *et al.* [14] and Maskery *et al.* [26].

However, other studies reported that the LPBF lattice structures can exhibit geometrical characteristics different from their original CAD data [13]. The SEM micrographs reveal that the lattice struts demonstrated rough surfaces (Figure 3) which could be due to semi-melted attached powder particles to the surfaces of the struts which could not be removed during the ultrasonic cleaning. Higher surface roughness and pores within the struts could have a detrimental effect on the mechanical properties of the lattice structures [7].

The samples were compressed uniaxially until mechanical failure occurs at the maximum load. The values of the applied load against displacement were recorded automatically with the MTS Criterion Model 43 Electric testing machine software. The Stress-strain graphs of compression test results are shown in Figure 4 and the resultant mechanical properties are presented in Table 2.

The general deformation of lattice structures can be divided into three categories. The linear elastic stage, plastics stage and densification stage [22]. During the linear elastic stage, the lattice structures deformed linearly, and its elastic modulus is proportional to the structure materials elastic modulus. Once the elastic limit is reached the cells begin to yield or buckle which represents the plastic deformation stage. The densification stage is reached when the cells make contact with each other and the stress increases steadily [22].

As can be observed from the stress-strain graphs the lattice structures demonstrated steady elastic deformation (Figure 4) as typical of lattice structures. However, the samples demonstrated limited plastic deformation and fail without going through the densification phase as postulated by previous authors [11,22,27]. This could be due to the magnitude of the load apply (30 kN). A similar elastic response of lattice structures was reported by de Damborenea *et al.* [6] without significant plastic and densification deformation before failure. Maskery *et al.* [26] also reported a similar observation for as-built LPBF lattice structures, however, after post heat treatment, the authors reported that the lattice structures underwent significant plastic and densification failure mechanism. For lattices structures once the plastic limit is reached, increasing the load would just result in a steady increase in the stress value due to densification while the mechanical integrity of the material is already compromised, hence the elastic and plastic stage deformations are the main characteristics that determined the selection of lattice structures for a particular application.

The mechanical properties of the rhombic and the diagonal lattice structures were almost the same, even though the geometrical and struts orientations are different. The similar results may be due to the same volume porosity and similar struts sizes. However, it is known that lattice structures with the same volume porosity with different geometrical struts orientations could produce entirely different mechanical property results (Table 3), which point to the fact that there are other parameters (cell type, cell geometry, orientation, etc.) apart from cell porosity that influences the mechanical properties of lattice structures.

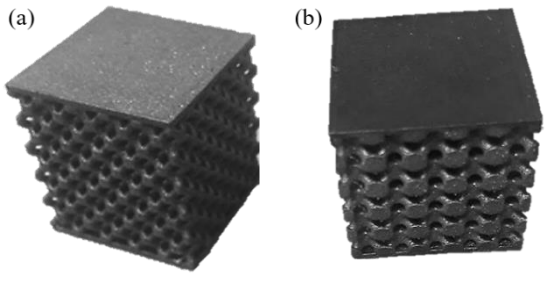

Figure 2. DMLS Ti6Al4V lattice structure: (a) rhombic and (b) diagonal.

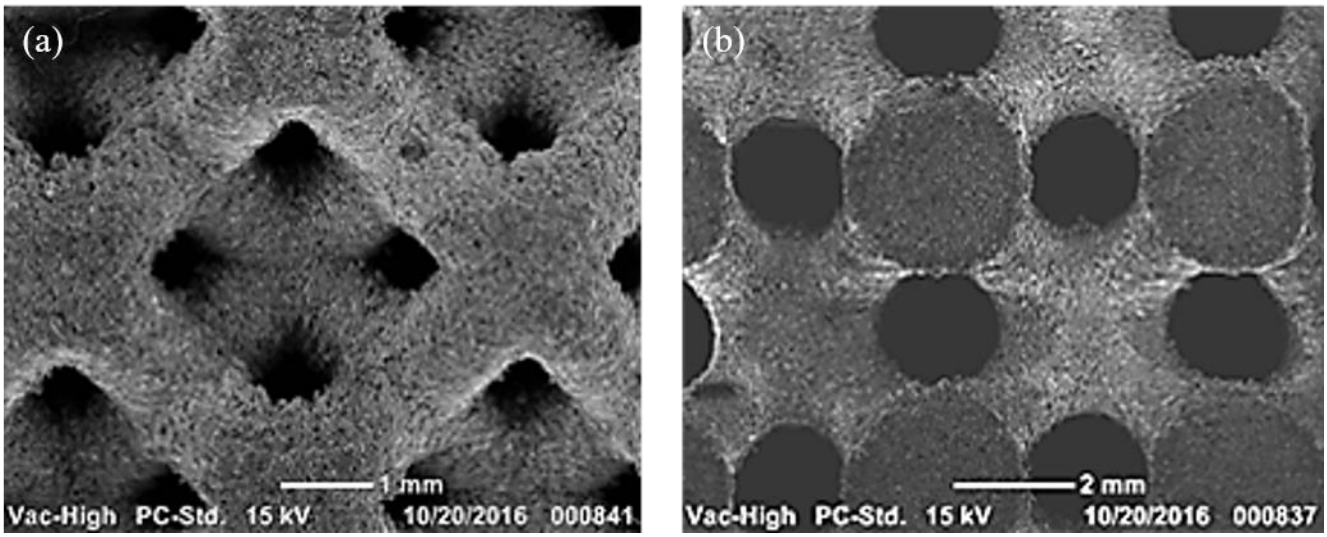

Figure 3. SEM micrographs of the struts of the Ti6Al4V lattice structure: (a) rhombic and (b) diagonal.

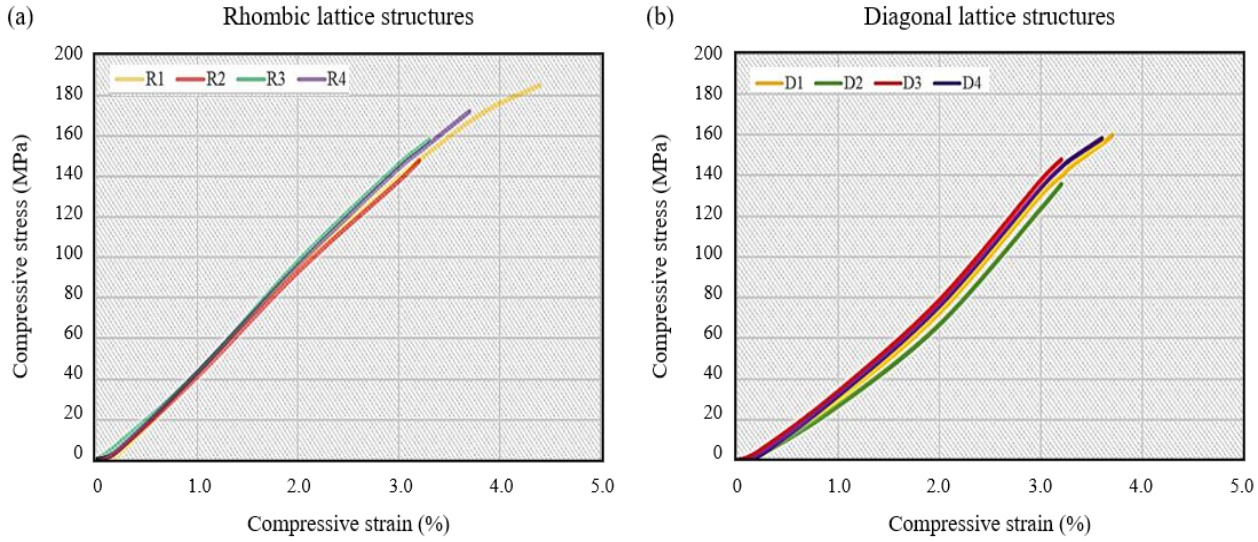

Figure 4. Compressive graph for Ti6Al4V lattice structures: (a) rhombic and (b) diagonal.

Table 2. Mechanical properties of LPBF Ti6Al4V lattice structures.

Types of lattice structure	Max load (kN)	Elastic Modulus (GPa)	Compressive stress at maximum load (MPa)	Compressive strain at maximum load (%)
Rhombic	25	5.3±0.2	168.4±14.4	3.40±0.58
Diagonal	25	5.1±0.1	162.7±4.8	3.19±0.07

Table 3. Mechanical properties of AM manufactured Ti6Al4V lattice structures.

Type of lattice structure	Porosity (%)	Elastic Modulus (GPa)	Ref.
Scaffold with rectangular struts	70.2±0.4	5.1±0.3	[11]
Scaffolds with shifted strut alignment	71.9±0.2	3.7±0.2	[11]
Scaffolds with diagonal struts	68.7±0.2	6.7±0.3	[11]
Unit cell in the form of prisms	69	0.341	[6]
Diamond structure	80.5	1.6	[28]
Hatched structure	59.5	12.9	[28]
Honeycomb-like structure	66.3	2.5	[29]

As can be observed from Table 3 the literature reveals a wide range of mechanical properties that could be obtained from Ti6Al4V lattice structures. The unique advantage of manipulating the mechanical properties of lattice structures based on the type of node, strut size, orientation, geometry, porosity, etc. have hinted the logical possibility of manufacturing biomedical and engineering products with tailored mechanical properties [31].

3.2 Microstructural analysis of the lattice structures

Metallic materials are highly microstructural sensitive, examining the microstructure of the lattice structures could reveal valuable information about its mechanical properties. Understanding the relationship between microstructure and properties of the lattice structures would empower the designing and manufacturing engineers to manipulate the mechanical properties of lattice structures for specific industrial applications [17].

The microstructures (Figure 5 and Figure 6) demonstrated the overlapping of subsequent scan tracks as a result of the optimum hatch distance and the selected scanning strategy employed, which signifies the perfect welding of each layer onto the layers that surround it. Such adequate overlapping would ensure the manufacturing of dense 3D lattice structures [23]. Further analysis reveals the presence of micropores, similar to what was reported by previous authors [5,14]. Maconachie *et al.* [22] pointed out that the micropores could be removed by post-thermal treatment. The micropores identified from the cross-section of the lattice struts were less than 20 µm when measured, hence the samples were considered as well-built dense 3D objects as reported elsewhere [32].

Due to the layer-wise (layer-by-layer) building process used by the LPBF technology the microstructure (Figure 5 and Figure 6) of the lattice's structures could be different when viewed from different planes (axial and radial axis). The cross-sections of the rhombic and diagonal nodes along the axial (perpendicular) axis reveal primary β with well-defined grain boundaries (Figure 5(a) and Figure 6(a)). The conspicuousness of the grain boundaries could be attributed to the complex crystallization environment during the LPBF process. The melting and solidification of the Ti6Al4V powder particles and the re-melting and re-solidification (thermal recycling) of the build platform produce an enabling environment for the formation of the well-defined grain boundaries. Columnar prior β grains were observed along the radial axis (along the build direction) of the cross-sections of the nodes (Figure 5(b) and Figure 6(b)). This is due to the epitaxial building methods used by the LPBF manufacturing technology [3,5]. Needles of fine acicular (α′) martensite were found inside the prior and columnar β grains. The martensitic formation is due to the inherent rapid rate of cooling and heating that accompanies the LPBF manufacturing process. The martensitic formation would lead to the production of LPBF as-built 3D components of low ductility [34]. This reduction in ductility due to the fast cooling rate might have contributed to the insignificant plastic deformation of the lattice structures before failure (Figure 4). The directional variation in the microstructure along the axial and radial directions is due to the very high rates of heating and cooling ($\sim 10^4$-10^6°C·s^{-1}) cum the solidification mechanisms [17] normally observed during the LPBF process.

It is also reported that the mechanical properties of LPBF samples are not isotropic along the axial and radial directions [5], due to the hydrodynamic movement of the melt flow and the rapid solidification mechanisms. To investigate this phenomenon of anisotropic behaviour of LPBF lattice structures, the microhardness of the samples were investigated along the axial and the radial directions. The FM-700 Digital Vickers Microhardness Tester at a constant load of 200 g for 15 s was used to make 15 indentations on the surface of the struts of each lattice structure and the average calculated. A microhardness value of 372±17 HV was recorded for the perpendicular direction (axial) and 361±12 HV along the building direction (radial). The difference in the microhardness values attest to the fact that LPBF build parts are not holistically homogenous throughout the bulk material as reported in the literature. The microhardness values of the current experiment correlate with the result of Becker *et al*. [5]. They investigated microstructural evolution and the mechanical properties of the LPBF Ti6Al4V parts under different heat treatment. For the as-built samples, a microhardness value of 367±5 HV was reported for the perpendicular (axial) direction and 354±6 HV for the built direction (radial).

3.3 Logical biomedical applications of the LPBF manufactured Ti6Al4V lattice structures

A careful study of nature had triggered the desire of exploring the benefit of lattice structures for various applications including biomedical applications [18]. Since nature is the most ideal model [9], then there is a need to mimic nature in manufacturing biomedical devices especially implanted devices with lattice structures.

Lattice structures are known to mimic the anisotropic porous nature of bone and the possibility of tuning their elastic modulus over a wide range by varying the lattice properties [35]. The creating of open space within the lattices would also translate to minimal material usage [10] and the discrete pore volumes in microns' dimensions would equally produce a perfect surface for bone-implant interlocking with suitable biomechanical properties [36]. The quest for the intense research into the mechanical properties of lattice structures for biomedical applications is driven by their ability to prevent stress shielding effect [12,37-39].

The mechanical properties analysis of the proposed LPBF Ti6Al4V lattice structures obtained from the current experiment are suitable for fabricating lightweight biomedical objects because their mechanical properties (Table 2) are close to the properties of human bone (Table 4).

A thorough review of the literature reveals a disparity results for elastic modulus for compact bone material, it ranges from 1-20 GPa [41-47]. This disparity might be due to the complex factors (age, gender, anatomical location, temperature, load orientation, amount of water present, geometry or architecture, arrangement of collagen fibers, mineral particles, bone density and bone diseases) that determined the mechanical properties of bones [49-51].

Nevertheless, the elastic modulus of the experimental lattice structures (Table 2) falls within the range of mechanical properties of cortical and cancellous bones. The mechanical properties of the lattice structures could be increased by changing the spatial configuration of the struts [27] of the lattice structures to obtain any desired required mechanical properties.

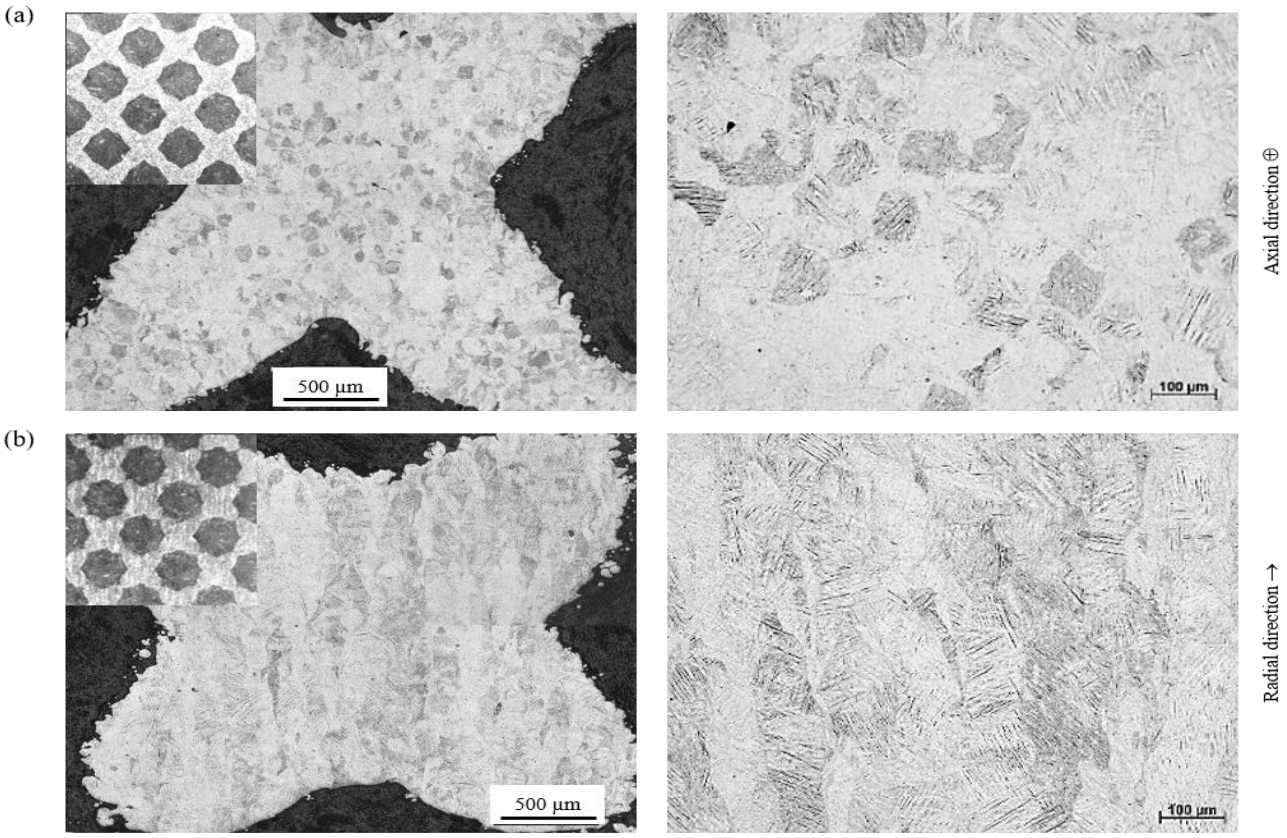

Figure 5. Microstructure of rhombic nodes: (a) axial direction and (b) radial direction.

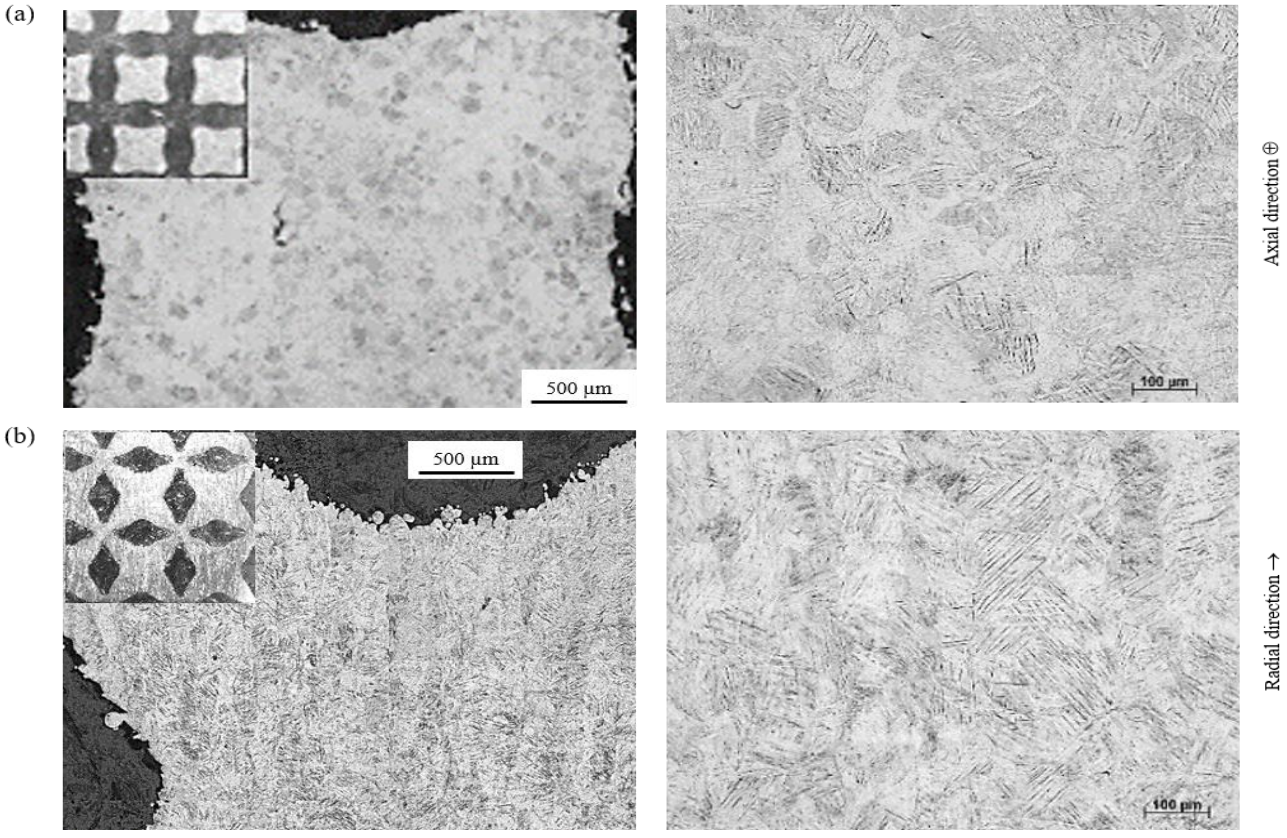

Figure 6. Microstructure of diagonal nodes: (a) axial direction and (b) radial direction.

As proven by nature (Figure 7) lattice structures can be used as structural biomedical material [9,52]. A cross-section of human bone morphology (Figure 7(a)), reveal a unique structure of solid-cellular-solid. Replacing damaged bones with solid-dense Ti6Al4V materials which have high elastic modulus (100-110 GPa [2]) would lead to a stress shielding effect. Biomimetic implants made out of cellular (lattice-non-stochastic cellular) objects would be more suitable. To avoid the stress shielding effect lattice structures of precise mechanical properties such as the once demonstrated in the current experiment must be used to replace damaged bone tissues. Implanted biomedical devices of low elastic modulus are recommended for areas of low bending stresses to ensure homogenous load transferred stress stimulation of the bone [12].

Such characteristics would serve the analogous function of epiphysis and metaphysis (Figure 7(a)) found in the human limbs [39]. Biomedical devices with low elastic modulus could stimulate the growth of bone cells due to mechanical stimulus by physiological load application [12].

The parietal cranial bone is part of the skull and its architectural arrangement is different from other parts of the skeletal system [54]. The skeletal systems have a cortical outer layer and cancellous inner part (Figure 7(a)). But parietal bone is made up of two outer cortical bone and sandwich cancellous bone (diploe Figure 7(b). Such an architectural arrangement of '*solid-porous-solid'* by nature would provide a lightweight structure that is capable of resisting damage under an external load of impact or crush. The spongy sandwich core serves as an intracranial channel and lightweight energy absorbing material while the solid cortical outer layer provides bending and share strength to the whole structure [55]. However, the current cranioplasty implants are completely solid or solid with some perforated holes [56] which do not synchronize with the natural architectural arrangement of the cranial bone structure. The recent review report of Kwarcinski *et al.* [57] has revealed that the dense solid cranial implants are most susceptible to implants infection when compared to less dense cranial implants. A biomimetic replacement is required for cranial traumatic patients to minimized implant failure. The response of the head to traumatic loading is intrinsically linked to the anatomy and mechanical properties of the crania [58,59], hence any replacement which does not comprehensively take necessary anatomical consideration in the design process could lead to implant failure. Lattice structures could be used to manufacture the '*solid-porous-solid'* architectural arrangement demonstrated by nature since their mechanical properties are similar to bone tissues.

Based on Figure 7(b), it could be predicted that during traumatic loading when the first outer cortical bone fractures the second still protects the brain before the cranial surgery, hence it is very important to produce biomimetic crania implants, especially in an era of high-speed automobiles. The automobile industry has taken advantage of the rapid advancement in technology and are producing vehicles that are moving with terrific speed resulting in increased accidents around the globe [60]. In case of damage to the head, it is very important to use biomimetic implants such as the one schematically presented in Figure 7(b), which can be manufactured using lattice structures. Such analogous replacement would prevent implant failure and improve the life of cranial implants patients.

The earlier technologies did not permit the manufacturing of biomimicry anatomical devices with control of mechanical properties. The conventional methods of manufacturing permit manufacturing of random cellular structures; a.k.a foams (stochastic structures) which limit the possibility of manufacturing 'porous structures' with tailored or control mechanical properties.

Table 4. Mechanical properties of adult human bones [44].

	Cortical bone		Cancellous bone
	Longitudinal direction	**Transverse direction**	
Tensile strength, MPa	79-151	51-56	
Compressive strength, MPa	131-224	106-133	2-5
Elastic moduli of bone, GPa	17-20	6-13	0.76-4

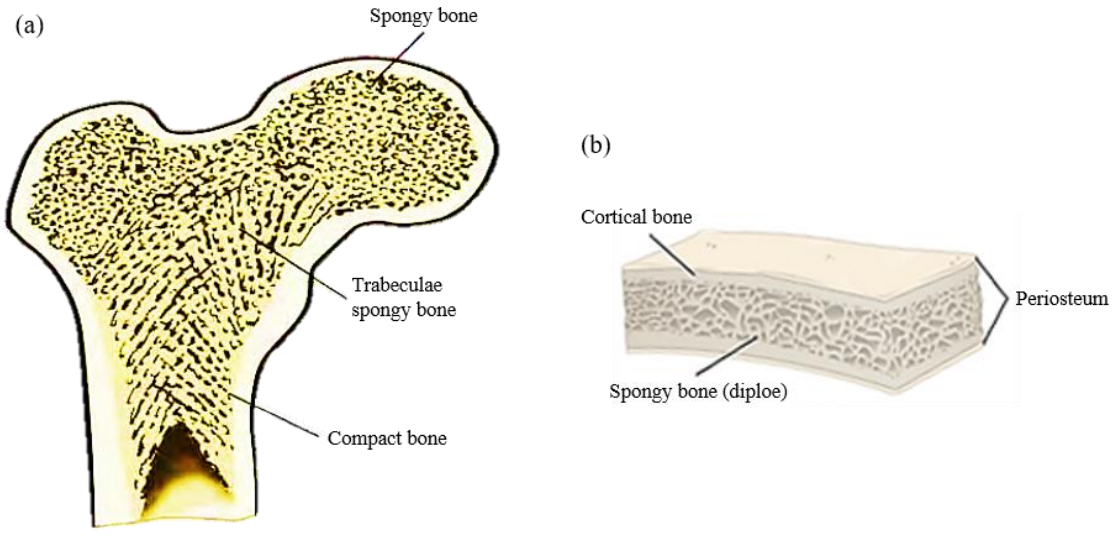

Figure 7. (a) Cross-section of bone [53] and (b) a schematic representation of the architectural arrangement of 'solid-porous-solid' of the skull.

However, with the advent of AM technologies such as at the LPBF manufacturing capability demonstrated in the current research, engineers can now produce structured foams (lattice structures) with control geometrical configuration and mechanical properties according to the desired specific function required - thus the possible manufacturing of biomedical devices such as implants with anatomical representations. Lattice structures can be customed design for optimum osseointegration due to their ability to sustain excellent bone ingrowth and high performance in terms of implant fixation.

It is also pointed out that lattice structures of the same struts size like foams are about 3 times stronger than a typical foam. The strength differences lie in the nature of material deformation. Foams are governed by cell wall bending, while lattice elements stretch and compress [10]. It could, therefore, be predicted that the next generational implants would probably be anatomical representative implants with lattice structures. It is not out of order when it is estimated that global demand for AM lattice structures for biomedical applications would grow to $116 billion by 2022 [61].

3.4 Logical engineering applications of the LPBF manufactured Ti6Al4V lattice structures

The quest to reduce the mass of aerospace and automobile parts to improve their performance is permanently in evolution. To this end, lightweight is the principal design objective in the aerospace and automobile industry. Because manufacturing such objects with lightweight structures like lattice structures would translate into the usage of less materials for manufacturing, less fuel consumption which also means less emission of NOx and higher performance enabling sustainable development at a lower cost [22]. It is widely speculated that for each kilogram of weight reduction in aircraft weight could save about US$ 3000 worth of fuel [62]. Huang *et al.* [63] went further to give a detailed breakdown of aircraft parts that can be manufactured by using the unique manufacturing advantages of AM. Using AM technologies to manufactured complex shapes such as lattice structures could lead to a 6.4% reduction in fuel consumption. NASA (National Aeronautics and Space Administration) reported that the application of lattice structures for aircraft manufacturing would lead to a 4.9% reduction in fuel consumption and an 8.3% reduction in NOx emissions [64,65]. The report of Bewlay *et al.* [66] also envisaged that using the AM technology to manufacture lightweight near-net shape of GEnx™ 1B (Boeing 787) and the GEnx™ 2B (Boeing 747-8) engine blades would probably lead to a 20% reduction in fuel consumption, a 50% reduction in noise, and an 80% reduction in NOx emissions compared with prior engines in its class whose engine blades were manufactured using the conventional methods of manufacturing. The possible advance in propulsion efficiency of aircraft would largely depend on the unique manufacturing capability of the AM technology to produced complex near-net shapes structures such as lattice structures.

The mechanical properties of the Ti6Al4V lattice structures (Table 2) produced in the current experiment perfectly fall within the range reported in the literature for most engineering applications [15,67-70]. Zhou *et al.* [67] produce lattice structure and obtained yield strength in the range of 91 MPa and 139 MPa which perfectly concord with the results of the current investigation. The lattice structures were used to manufacture lightweight phase-change thermal controllers to manage the temperature of various electronics in spacecraft. The thermal controllers demonstrated high efficiency of a 50% increase in thermal capacity compared to traditional alternatives with similar mass. The architectural design of lattice structures could provide the advantage of a large surface area and a large number of interconnected pores to produce an optimized heat transfer system for most engineering applications.

Obviously, with the monolithic manufacturing capabilities of LPBF, AM is now at the center stage of manufacturing technology to revolutionize the manufacturing industry. The conventional methods of manufacturing could be used to produce only foams (stochastic structures) but cannot easily produce periodic array to enables the manufacturing engineer to produce lattice structures with reliable and reproducible mechanical properties. The LPBF manufacturing process has enabled unprecedented design flexibilities and application opportunities. Lattice structures possess many superior properties to solid material and conventional structures. Lattice structures are able to integrate more than one function into a physical part [68,69], which makes it attractive to a wide range of applications. With the unique capability of the LPBF manufacturing technology to produce lattice structures with complex geometrical accuracy, the era of producing next generational biomedical devices with biomimetic architecture and engineering products with tailored mechanical properties based on the geometrical and functional requirements of the components has arrived.

4. Conclusions

LPBF manufacturing technology was used to produced lattice structures using rhombic and diagonal nodes. The mechanical properties of the diagonal (5.1±0.1 GPa) and rhombic (5.3±0.2 GPa) lattice structures could be used to produce biomedical implants with low elastic modulus which could prevent stress shielding effects. The lightweight properties of the lattice structures with its multifunctional capabilities also make them very suitable for use in the aircraft and automobile industries and other engineering applications.

Acknowledgements

This work is based on the research supported by the South African Research Chairs Initiative of the Department of Science and Technology and National Research Foundation of South Africa (Grant No. 97994). The author would like to acknowledge the contribution of Prof. I. Yadroitsau, Prof. P. Krakhmalev and Dr. I. Yadroitsava who were his doctoral studies supervisors.

References

[1] V. Jablokov, M.J. Nutt, M. Richelsoph, and H.L. Freese, “The application of Ti-15Mo beta titanium alloy in high strength structural orthopaedic applications"*In Titanium, Niobium, Zirconium, and Tantalum for Medical and Surgical Applications*, ASTM International, 2006.

[2] M. Niinomi, Y. Liu, M. Nakai, H. Liu, and Li, H, "Biomedical titanium alloys with Young's moduli close to that of cortical bone," *Regenerative biomaterials*, vol. 3(3), pp.173-185, 2016.

[3] T. Becker, M. Beck, and C. Scheffer, "Microstructure and mechanical properties of direct metal laser sintered Ti-6AL-4V," *South African Journal of Industrial Engineering*, vol. 26(1), pp. 1-10, 2015.

[4] L. Thijs, F. Verhaeghe, T. Craeghs, J. Van Humbeeck, and J.P. Kruth, "A study of the microstructural evolution during selective laser melting of Ti–6Al–4V," *Acta Materialia*, vol. 58(9), pp. 3303-3312, 2010.

[5] T. Becker, M. Van Rooyen, and D. Dimitrov, "Heat treatment of Ti-6Al-4V produced by lasercusing," *South African Journal of Industrial Engineering*, vol. 26(2), pp. 93-103, 2015.

[6] J.J. de Damborenea, M.A. Larosa, M.A. Arenas, J.M. Hernández-López, A.L. Jardini, M.C.F. Ierardi, C.A. Zavaglia, R. Maciel Filho, and A. Conde, "Functionalization of Ti6Al4V scaffolds produced by direct metal laser for biomedical applications," *Materials & Design*, vol. 83, pp. 6-13, 2015.

[7] M. Zhang, Z. Yang, Z. Lu, B. Liao, and X. He, "Effective elastic properties and initial yield surfaces of two 3D lattice structures," *International Journal of Mechanical Sciences*, vol. 138, pp. 146-158, 2018.

[8] H. Gu, M. Pavier, and A. Shterenlikht, " Experimental study of modulus, strength and toughness of 2D triangular lattices," *International Journal of Solids and Structures*, vol. 152, pp. 207-216, 2018.

[9] L.J. Gibson, and M.F. Ashby, *Cellular solids: structure and properties*, Cambridge: University Press, Cambridge, UK., 1997.

[10] D.W. Rosen, S.R. Johnston, and M. Reed, "*Design of general lattice structures for lightweight and compliance applications*," 2006.

[11] J. Wieding, A. Jonitz, and R. Bader, "The effect of structural design on mechanical properties and cellular response of additive manufactured titanium scaffolds," *Materials*, vol. 5(8), pp. 1336-1347, 2012.

[12] T.C. Dzogbewu, " Additive manufacturing of porous Ti-based alloys for biomedical applications–a review," *Journal for New Generation Sciences*, vol. 15(1), pp. 278-294, 2017.

[13] N. Tanlak, D.F. De Lange, and W. Van Paepegem, "Numerical prediction of the printable density range of lattice structures for additive manufacturing," *Materials & Design*, vol. 133, pp. 549-558, 2017.

[14] Z. Ma, D.Z. Zhang, F. Liu, J. Jiang, M. Zhao, and T. Zhang, "Lattice structures of Cu-Cr-Zr copper alloy by selective laser melting: Microstructures, mechanical properties and energy absorption," *Materials & Design*, pp. 108406, 2019.

[15] W. Tao and M.C. Leu, "Design of lattice structure for additive manufacturing," in *International Symposium on Flexible Automation (ISFA)*, Cleveland, Ohio, U.S.A., 2016.

[16] M.C. Messner, "Optimal lattice-structured materials," *Journal of the Mechanics and Physics of Solids*, vol. 96, pp. 162-183, 2016.

[17] T.C. Dzogbewu, *Direct metal laser sintering of titanium alloys for biomedical applications*, Doctoral dissertation-Central University of Technology, Free State, 2017.

[18] M.F. Ashby, A. Evans, N.A. Fleck, L.J. Gibson, J.W. Hutchinson, H.N.G. Wadley, and F. Delale, *Metal foams: a design guide*, Woburn: Butterworth-Heinemann, 2001.

[19] H. Fan, F. Jin, and D. Fang, "Characterization of edge effects of composite lattice structures," *Composites Science and Technology*, vol. 69(11), pp. 1896-1903, 2009.

[20] EOS, "*EOS Titanium Ti64*," EOS GmbH - Electro Optical Systems, 2014.

[21] ISO 13314 "*Mechanical Testing of Metals. Ductility Testing. Compression Test for Porous and Cellular Metals*," ISO: Geneva, Switzerland.

[22] T. Maconachie, M.L.B.Z.X. Leary, M. Qian, O. Faruque, and M. Brandt, "SLM lattice structures: Properties, performance, applications and challenges," *Materials & Design*, pp. 108137, 2019.

[23] T.C. Dzogbewu, "Laser powder bed fusion of Ti15Mo," *Results in Engineering*, pp.100155, 2020.

[24] T.C. Dzogbewu, I. Yadroitsev, P. Krakhmalev, I. Yadroitsava, and A. Du Plessis, "Optimal process parameters for in-situ alloyed Ti15Mo structures by Direct Metal Laser Sintering," in *The Twenty-Eighth Annual International Solid Freeform Fabrication (SFF) Symposium – An Additive Manufacturing Conference*, The University of Texas, Austin , 2017.

[25] I. Yadroitsev, I. Shishkovsky, P. Bertrand, and I. Smurov, "Manufacturing of fine-structured 3D porous filter elements by selective laser melting," *Applied Surface Science*, vol. 255(10), pp. 5523-5527, 2009.

[26] I. Maskery, N.T. Aboulkhair, A.O. Aremu, C.J. Tuck, I.A. Ashcroft, R.D. Wildman, and R. J. Hague, "A mechanical property evaluation of graded density Al-Si10-Mg lattice structures manufactured by selective laser melting," *Materials Science and Engineering: A*, vol. 670, pp. 264-274, 2016.

[27] N. Contuzzi, S.L. Campanelli, C. Casavola, and L. Lamberti, "Manufacturing and Characterization of 18Ni Marage 300 Lattice Components by Selective Laser Melting," *Materials*, vol. 6(8), pp. 3451-3468, 2013.

[28] P. Heinl, L. Müller, C. Körner, R.F. Singer, and F.A. Müller, "Cellular Ti–6Al–4V structures with interconnected macro porosity for bone implants fabricated by selective electron beam melting," *Acta biomaterialia*, vol. 4(5), pp. 1536-1544, 2008.

[29] X. Li, C. Wang, W. Zhang, and Y. Li, " Fabrication and characterization of porous Ti6Al4V parts for biomedical applications using electron beam melting process," *Materials Letters*, vol. 63(3), pp. 403-405, 2009.

[30] J. Parthasarathy, B. Starly, S. Raman, and A. Christensen, "Mechanical evaluation of porous titanium (Ti6Al4V) structures with electron beam melting (EBM)," *Journal of the mechanical behavior of biomedical materials*, vol. 3(3), pp. 249-259, 2010.

[31] T.C. Dzogbewu, L. Monaheng, I. Yadroitsava, W.B. du Preez, and I. Yadroitsev, "Finite element analysis in design of DMLS mandible implants", *In Challenges for Technology Innovation (vol. 155(160), pp. 155-160)*. ROUTLEDGE in association with GSE Research.

[32] E. Abele, H.A. Stoffregen, K. Klimkeit, H. Hoche, and M. Oechsner, "Optimisation of process parameters for lattice structures," *Rapid Prototyping Journal*, vol. 21(1), pp. 117-127, 2015.

[33] T.B. Kim, S. Yue, Z. Zhang, E. Jones, J.R. Jones, and P. D. Lee, "Additive manufactured porous titanium structures: Through-process quantification of pore and strut networks," *Journal of Materials Processing Technology*, vol. 214(11), pp. 2706-2715, 2014.

[34] M. Thöne, S. Leuders, A. Riemer, T. Tröster and H. A. Richard, "Influence of heat-treatment on selective laser melting products–eg Ti6Al4V," in *In Solid Freeform Fabrication Symposium SFF, Austin, Texas.*, 2012.

[35] P. Soman, J. W. Lee, A. Phadke, S. Varghese and S. Chen, "Spatial tuning of negative and positive Poisson's ratio in a multi-layer scaffold," *Acta biomaterialia*, vol. 8(7), pp. 2587-2594, 2012.

[36] M. Mour, D. Das, T. Winkle, E. Hoenig, G. Mielke, M. M. Morlock and A. F. Schilling, "Advances in Porous Biomaterials for Dental and Orthopaedic Applications," *Materials*, vol. 3(5), pp. 2947-2974, 2010.

[37] A.Í.S. Antonialli, and C. Bolfarini, "Numerical evaluation of reduction of stress shielding in laser coated hip prostheses," *Materials Research*, vol. 14(3), pp. 331-334, 2011.

[38] M. Niinomi, and M. Nakai, "Titanium-based biomaterials for preventing stress shielding between implant devices and bone," *International journal of biomaterials*, vol. 2011, pp. 10, 2011.

[39] H. Liu, and T.J. Webster, "Bioinspired nanocomposites for orthopedic applications," *Nanotechnology for the Regeneration of Hard and Soft Tissues*, pp. 8, 2007.

[40] A. Nouri, P.D. Hodgson, and C. E. Wen, "Biomimetic porous titanium scaffolds for orthopedic and dental applications," *Biomimetics learning from nature*, pp. 415-450, 2010.

[41] J.Y. Rho, R.B. Ashman, and C.H. Turner, "Young's modulus of trabecular and cortical bone material: ultrasonic and microtensile measurements," *Journal of biomechanics*, vol. 26(2), pp. 111-119, 1993.

[42] R.B. Ashman and J. Y. Rho, "Elastic modulus of trabecular bone material," *Journal of biomechanics*, vol. 21(3), pp. 177-181, 1988.

[43] J.L. Kuhn, S.A. Goldstein, R. Choi, M. London, L.A. Feldkamp, and L.S. Matthews, "Comparison of the trabecular and cortical tissue moduli from human iliac crests," *Journal of orthopaedic research*, vol. 7(6), pp. 876-884, 1989.

[44] P.L. Mente, and J.L. Lewis, "Experimental method for the measurement of the elastic modulus of trabecular bone tissue," *Journal of Orthopaedic Research*, vol. 7(3), pp. 456-461, 1989.

[45] K. Choi, J.L. Kuhn, M.J. Ciarelli, and S.A. Goldstein, "The elastic moduli of human subchondral, trabecular, and cortical bone tissue and the size-dependency of cortical bone modulus," *Journal of biomechanics*, vol. 23(11), pp. 1103-1113, 1990.

[46] C.G.M. Pezowicz, "The mechanical properties of human ribs in young adult," *Acta of Bioengineering and Biomechanics*, vol. 14(2), 2012.

[47] C. Öhman, M. Baleani, C. Pani, F. Taddei, M. Alberghini, M. Viceconti, and M. Manfrini, "Compressive behaviour of child and adult cortical bone," *Bone*, vol. 49(4), pp. 769-776, 2011.

[48] C.E. Hoffler, K.E. Moore, K. Kozloff, P.K. Zysset, and S.A. Goldstein, "Age, gender, and bone lamellae elastic moduli," *Journal of Orthopaedic Research*, vol. 18(3), pp. 432-437, 2000.

[49] M.A. Velasco, C.A. Narváez-Tovar, and D.A. Garzón-Alvarado, "Design, materials, and mechanobiology of biodegradable scaffolds for bone tissue engineering," *BioMed research international*, vol. 2015, 2015.

[50] A.T. Jang, J.D. Lin, R.M. Choi, E.M. Choi, M.L. Seto, M.I. Ryder, S.A. Gansky, D.A. Curtis. and S.P. Ho, "Adaptive properties of human cementum and cementum dentin junction with age," *Journal of the mechanical behavior of biomedical materials*, vol. 39, pp. 184-196, 2014.

[51] C.E. Hoffler, K.E. Moore, K. Kozloff, P.K. Zysset, M.B. Brown, and S.A. Goldstein, "Heterogeneity of bone lamellar-level elastic moduli," *Bone*, vol. 26(6), pp. 603-609, 2000.

[52] U.G. Wegst, H. Bai, E. Saiz, A.P. Tomsia, and R.O. Ritchie, "Bioinspired structural materials," *Nature materials*, vol. 14(1), pp. 23-36, 2015.

[53] A.D.P. Bankoff, "Biomechanical Characteristics of the Bone, Human Musculoskeletal Biomechanics" Dr. Tarun Goswami (Ed.), ISBN: 978-953-307-638-6, InTech, Available from: http://www.intechopen.com/books/human-musculoskeletal-biomechanics/biomechanical-characteristics-of-thebone.

[54] J.H. McElhaney, J.L. Fogle, J.W. Melvin, R.R. Haynes, V.L. Roberts, and N.M. Alem, "Mechanical properties of cranial bone," *Journal of biomechanics*, vol. 3(5), pp. 495IN5497-496511, 1970.

[55] D.B. Burr, and M.R. Allen, *Basic and applied bone biology*, Academic Press, 2013.

[56] S. Aydin, B. Kucukyuruk, B. Abuzayed, S. Aydin, and G.Z. Sanus, "Cranioplasty: review of materials and techniques," *Journal of neurosciences in rural practice*, vol. 2(2), pp. 162, 2011.

[57] J. Kwarcinski, P. Boughton, A. Ruys, A. Doolan, and J. Van Gelder, "Cranioplasty and craniofacial reconstruction: a review of implant material, manufacturing method and infection risk," *Applied sciences*, vol. 7(3), pp. 276, 2017.

[58] J.H. McElhaney, J.L. Fogle, J.W. Melvin, R.R. Haynes, V.L. Roberts, and N.M. Alem, "Mechanical properties of cranial bone," *Journal of biomechanics*, vol. 3(5), pp. 495IN5497-496511, 1970.

[59] M. Cammarata, F. Nicoletti, M. Di Paola, A. Valenza, and G. Zummo, "Mechanical behavior of human bones with different saturation levels," *MDPI*, 2016.

[60] H. Worley, "*Road traffic accidents increase dramatically worldwide*," Population reference bureau, 2015.

[61] A.M. Research, "*Medical Implants Market Size, Share | Industry Analysis 2022*," 2019. [Online]. Available: https://www.alliedmarketresearch.com/medical-implants-market. [Accessed 01 2020].

[62] J. Coykendall, M. Cotteleer, J. Holdowsky, and M Mahto,"3D opportunity in aerospace and defense: Additive manufacturing takes flight," *A Deloitte series on additive manufacturing,1*, 2014.

[63] R. Huang, M. Riddle, D. Graziano, J. Warren, S. Das, S. Nimbalkar, J. Cresko and E. Masanet, "Energy and emissions saving potential of additive manufacturing: the case of lightweight aircraft components," *Journal of Cleaner Production*, vol. 135, pp. 1559-1570, 2016.

[64] B. Haller, "*NASA's vision for potential energy reduction from future enerations of propulsion technology*," National Aeronautics and Space Administration, 2015.

[65] S. Singamneni, L. V. Yifan, A. Hewitt, R. Chalk and W. Thomas, "Additive Manufacturing for the Aircraft Industry: A Review," *Journal of Aeronautics & Aerospace Engineering*, vol. 8(1), 2019.

[66] B. P. Bewlay, M. Weimer, T. Kelly, A. Suzuki and P. R. Subramanian, "The science, technology, and implementation of TiAl alloys in commercial aircraft engines," *MRS Online Proceedings Library Archive*, vol. 1516, pp. 49-58, 2013.

[67] J. Zhou, P. Shrotriya and W. O. Soboyejo, "On the deformation of aluminum lattice block structures: from struts to structures," *Mechanics of Materials*, vol. 36(8), pp. 723-737, 2004.

[68] M. Bici, S. Brischetto, F. Campana, C. G. Ferro, C. Seclì, S. Varetti, P. Maggiore and A. Mazza, "Development of a multifunctional panel for aerospace use through SLM additive manufacturing," *Procedia CIRP*, vol. 67, pp. 215-220, 2018.

[69] C. G. Ferro, S. Varetti, G. De Pasquale and P. Maggiore, "Lattice structured impact absorber with embedded anti-icing system for aircraft wings fabricated with additive SLM process," *Materials Today Communications*, vol. 15, pp. 185-189, 2018.

[70] Z. H. O. U. Hao, X. Zhang, Z. E. N. G. Huizhong, Y. A. N. G. Huning, L. E. Hongshuai, L. I. Xiao and W. A. N. G. Yaobing, "Lightweight structure of a phase-change thermal controller based on lattice cells manufactured by SLM," *Chinese Journal of Aeronautics*, vol. 32(7), pp. 1727-1732, 2019.